

Natural Expression of Physical Models of Impossible Figures and Motions

Mimetic Surface Color and Texture Adjustment (MSCTA)

Tsuruno, Sachiko
Kindai University
sachiko@fuk.kindai.ac.jp

Abstract

Two-dimensional (2D) drawings of impossible figures are typified by the lithographs of the Dutch artist M.C. Escher, such as “Waterfall,” “Belvedere,” and “Ascending and Descending.” Impossible figures are mental images of solid objects. In other words, a three-dimensional (3D) figure that is visualized intuitively from a 2D drawing of an impossible figure cannot be constructed in 3D space. Thus, in reality, a 3D model of an impossible figure has an unexpectedly disconnected or deformed structure, but the 3D figure corresponds to the 2D figure from a specific viewpoint, although not from other viewpoints. Methods for representing 3D models of impossible figures have been studied in virtual space. The shapes and structures of impossible object have also been studied in real space, but the effects of physical illumination by light and appropriate textures have not been considered. Thus, this paper describes the mimetic surface color and texture adjustment (MSCTA) method for producing naturally shaded and appropriately textured 3D impossible objects under physical light sources. And some creative works applying this method are shown, including a new structure with impossible motion.

Keywords: impossible figure, impossible motion, physical object

1 Introduction

1.1 Early Impossible Figure

Artwork featuring impossible figures dates back to 1568. In the painting *The Magpie on the Gallows* by Bruegel, the structure of the gallows is an impossible rectangle. In 1754, W. Hogarth painted *Satire on False Perspective*. Reutersvard drew an impossible tribar consisting of nine cubes in 1934 and went on to draw many other impossible figures^[1]. L.S. and R. Penrose published visual illusions of an impossible tribar and an impossible staircase^[2]. Around that time, M.C. Escher created some lithographs that used impossible figures as a motif^[3]. Although he later gained fame as an artist, his lithographs initially attracted interest from scientific fields.

1.2 Investigation of Impossible Figures

Impossible figures have been studied in psychology^{[4]-[7]}, and in mathematics and computer science^{[8]-[22]}. Based on these researches, various expressions of impossible figures have become possible by means of computer graphics. Simanek provided false perspective drawings and stereo pair drawings of impossible figures^[23]. Tsuruno used animation to present Escher's *Belvedere* from novel angles^[24]. Khoh and Kovesi proposed line drawing animation of impossible rectangles by using two complementary halves^[25]. Savransky et al. proposed how impossible three-dimensional scenes were modeled and rendered synthetically^[26]. Owada and Fujiki

generated a modeling system to combine multiple 3D parts in a projected 2D domain^[27]. Orbons and Ruttkay appeared physically correct, but are connected in an impossible manner, similar to *Escher's Another World II or Relativity*^[28]. Wu et al. automatically generated an optimized view-dependent 3D impossible model from a set of a figure's 3D locally possible parts^[29]. Elber presented a regular 3D model that could be converted to an impossible model by applying line of sight deformations^[30].

1.3 Peculiarity of 3D Impossible Figures

Impossible figures are mental images of solid objects: viewers perceive the 2D drawing as a 3D structure, but intuitively recognize that it cannot be realized in 3D space. For example, when viewers look at a drawing like the one shown in Figure 1, they recognize intuitively that the four corners are each composed of right angles but it is impossible to build such an object in 3D space. To construct an impossible figure in 3D space, the structure must be disconnected as shown in Figure 2 or deformed as shown in Figure 3. In other words, from one specified viewpoint, the 3D figure corresponds to the 2D, but from other viewpoints, the 3D figure appears disconnected or deformed. For the unconnected model, the directions of each surface that the viewer intuitively recognizes are the same as the real surface directions, as shown in Figure 2(2). So, the shading of the figure in Figure 2(1) appears natural. The connected model must be deformed, so each surface is facing

in an unexpected direction as shown in Figure 3(3) and (4), and the shading of the figure causes the viewer to feel a sense of incongruity as shown in Figure 3(1). The object's color appears graduated despite the monochromatic shade of white. The texture-mapped object in Figure 3(2) appears even more unnatural. When displayed on a 2D computer screen or printed on paper, the figure can be solved by the normals used for shading being sampled from the corresponding unconnected model. But this method is not available for a 3D model fabricated as a physical object. We solve this problem by using our new method.

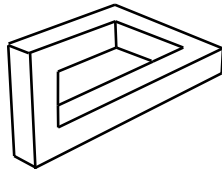


Figure 1: Line drawing of an impossible figure.

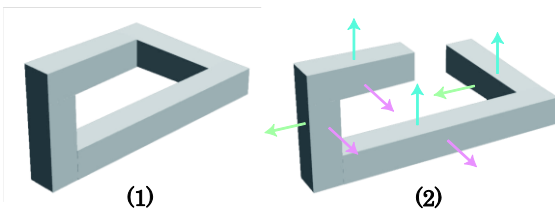


Figure 2: Rendering of an unconnected model: (1) from a specified viewpoint, (2) from a different angle.

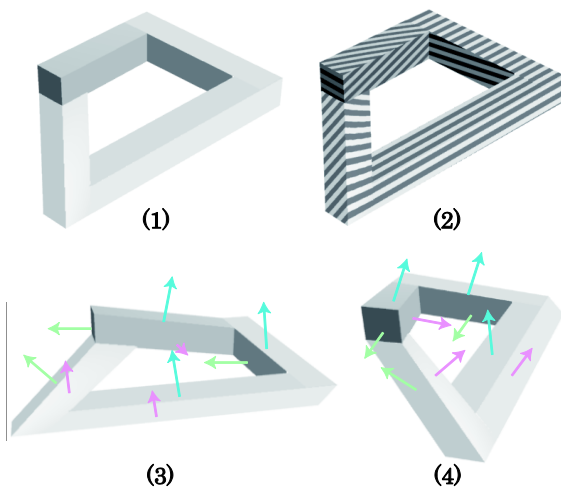


Figure 3: Rendering of a connected model: (1) from a specified viewpoint, (2) texture-mapped model from a specified viewpoint, (3) from a different angle, (4) from another different angle.

2 Related Work

2.1 Related Papers

Sugihara formulated the algebraic structure of the degrees of freedom of a 3D polyhedron projected onto a 2D screen as a congruent figure^{[16][17]}. This concept for shape modeling of impossible figures is adopted here. However, Sugihara gave no description of rendering impossible models. Renderings a

connected model of an impossible figure has been described in the following papers. Wu et al. rendered impossible figures using directional lighting and point-source lighting with variable viewpoint changes. In addition, they applied an isotropic bidirectional reflectance distribution function and re-rendered it in a distant environment. The shaded surface looked natural even when the model had been severely deformed^[29]. However, the normals used for rendering were sampled from the original 3D model. Elber performed modeling by means of line of sight deformations and rendered natural-looking 3D impossible models. Elber also used the original vertex normals of the object before the deformation for rendering^[30]. Therefore, the methods of Wu et al. and Elber are not available for physical 3D models.

2.2 Related Physical 3D Objects and Impossible Motion

Many artists and scientists have presented impossible figures in real 3D space. Fukuda realized the building depicted in Escher's prints *Belvedere* in 1982 and *Waterfall* in 1985^[1]. Hamaekers sculpted an impossible cube and Penrose triangles out of painted wood and polyester in 1984^[1]. Moretti has created transforming sculptures with orthogonal intersection since 1997^[1]. Sugihara^[15] used paper to construct various impossible objects including unique figures based on his mathematical picture-interpretation theory. Lipson built impossible figures out of LEGO bricks^[31]. Elber created physical models that were designed and built using geometric modeling and computer graphics tools for impossible figures^[32]. The magician Tabary created sculptures of impossible figures^[33].

About impossible motion, Sugihara presented Magnet-like Slopes^[34]. On four slopes in a cross-like arrangement that appear to meet at an apex, wooden balls seem to move against gravity. In actuality each slope is downward, but by placement of a deformed slope, it is erroneously seen as an uphill slope.

All models mentioned above were photographed to make the unnaturalness inconspicuous, and the effects of physical illumination by light sources and appropriate textures have not been considered. Tsuruno presented impossible motion with textured impossible models at a contest^[35], but the technique has not been published.

3 Method for Natural Shading and Appropriate Texture Mapping

3.1 Mimetic Surface Color and Texture Adjustment

When two figures are located on exactly the same line of sight, as shown in Figure 4, the projected line drawings of the two figures can be identical. However, the two projected shaded drawings are not recognized as identical. For example, the apparent object *A* in Figure 5 and the mimetic object *M* in Figure 6 are different. However, the projected line drawings of *A* and *M* are identical in Figures 5(3) and 6(3). When objects *A* and *M* are shaded as usual, *A* and *M* that are the same color appear different, as shown in Figures 5(4) and 6(4). Figures

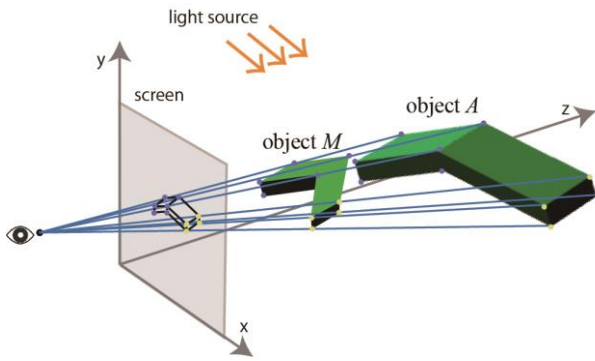


Figure 4: Two figures on the same line of sight.

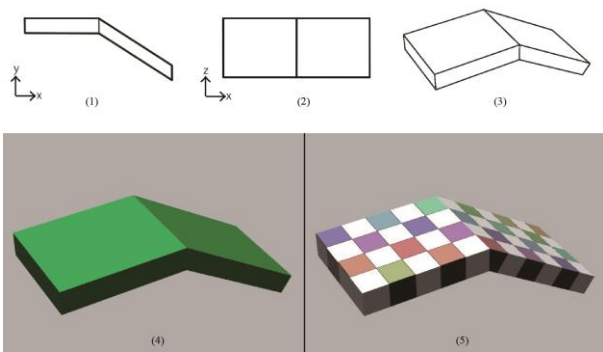


Figure 5: Apparent object A: (1) front view, (2) top view, (3) projected line drawing, (4) projected shaded drawing, (5) projected texture-mapped drawing.

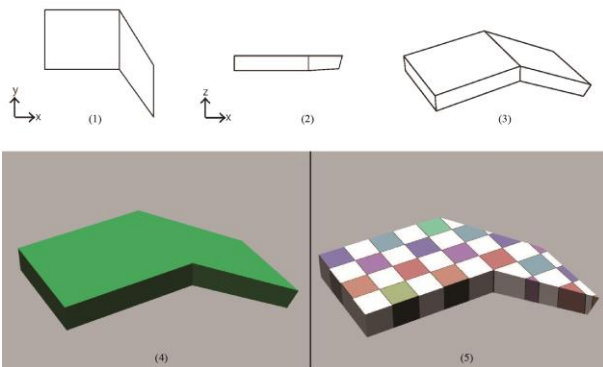


Figure 6: Mimetic object M: (1) front view, (2) top view, (3) projected line drawing, (4) projected shaded drawing, (5) projected texture-mapped drawing.

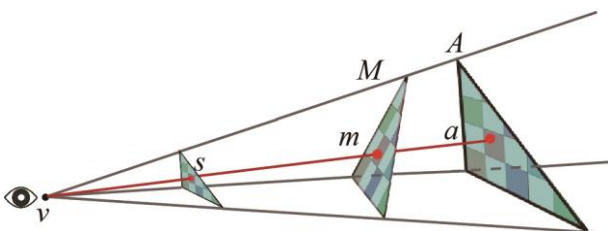


Figure 7: Color and texture adjustment.

5(5) and 6(5) show that when objects A and M are texture-mapped, the difference between them is usually more pronounced than that when they are the single color.

If shaded M can be made to appear the same as shaded A, this method can also be applied to impossible figures. For virtual models on a computer screen, when object M is rendered, the normals obtained from object A can be used for shading, instead of those from object M. However, this is not possible for real 3D models because physical light sources are present. Therefore, to give M the same appearance as A in real space, the original object color of M must be changed. In other words, we need to find the appropriate original color of object M to make it resemble object A in certain lighting conditions.

In Figure 7, A is an apparent surface, M is a mimetic surface, a is a point on surface A, m is a point on surface M, and v is the camera position. Points a, m, and v are collinear. Let I_a and I_m be the intensity of reflection at points a and m, respectively. Let C_a and C_m be the object colors at a and m, respectively. Each RGB color component ranges from 0 to 1. C_m is given by

$$C_m = \frac{I_a}{I_m} C_a \quad (1)$$

where C_a , I_a , and I_m are restricted to yielding the RGB components of C_m in a range from 0 to 1. This calculation is applied to every point on surface M, thereby determining the original color of surface M. This method is applicable to a texture-mapped surface. We refer to this method as *mimetic surface color and texture adjustment (MSCTA)*. Figure 8 illustrates the result obtained after applying MSCTA to the object in Figure 6. Figure 9 shows a view from a different angle for comparison. A directional light source is used for shading in Figures 5, 6, 8, and 9.

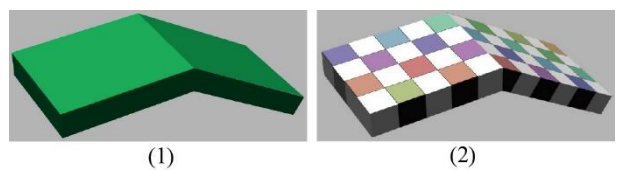


Figure 8: Result of applying MSCTA to shaded object M in Figure 6.

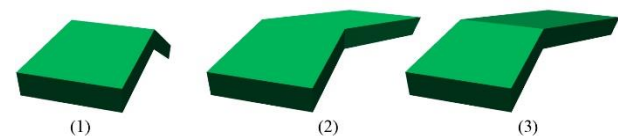


Figure 9: From a different angle: (1) apparent object A, (2) mimetic object M, (3) mimetic object M applying MSCTA.

3.2 Limitation

During impossible motion, moving physical balls need to be placed on the mimetic object. In this case, deformed specular reflections are formed and deformed shadows are cast by the moving physical balls on the mimetic surfaces. Thus, real world specular materials are not used, which is why specular reflection is not calculated. In addition, according to a survey regarding the deformed shadows cast on the mimetic surface in

our study, none of the observers noticed that the shadows were deformed. Therefore, no measures were taken to deal with shadows on the mimetic surface in the present study. The mimetic surfaces cast deformed shadows on the background, but they were made less noticeable by using a black background. Consequently, the results of the computation were sufficiently effective for our creative works, even given this limitation.

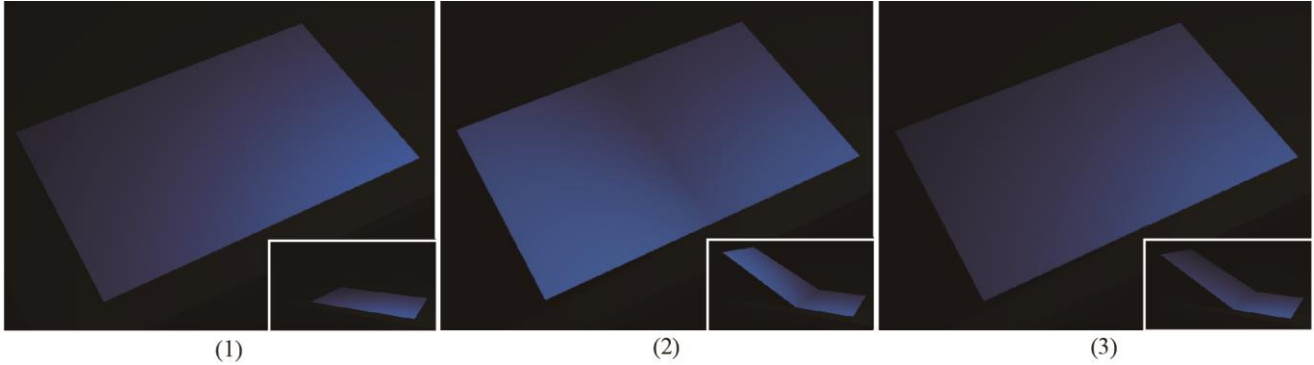


Figure 10: A point light source is used. A comparison among the following: (1) apparent surface, (2) the mimetic surface before applying MSTCA, (3) the mimetic surface after applying MSTCA. Each inset in the lower right shows the plate viewed from a different angle

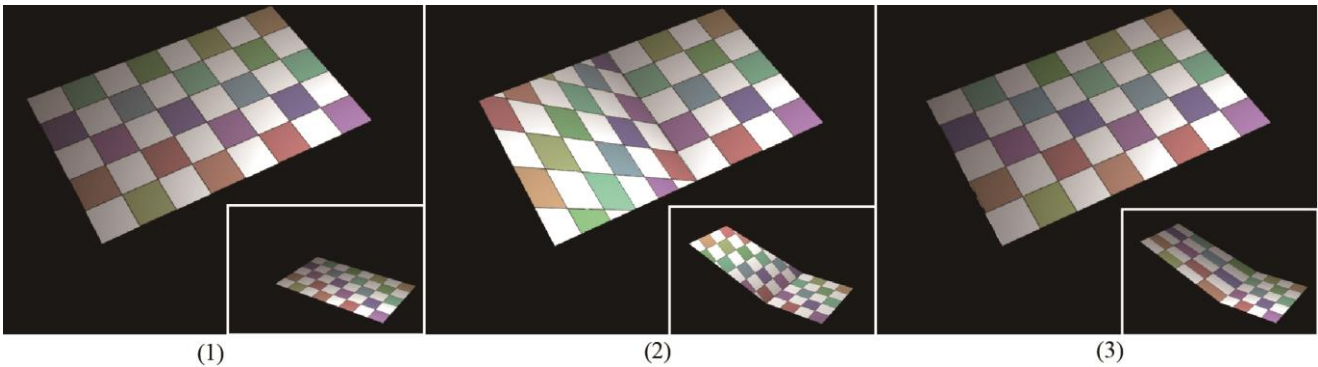


Figure 11: Each plate is texture-mapped under a point light source. A comparison among the following: (1) apparent surface, (2) the mimetic surface before applying MSTCA, (3) the mimetic surface after applying MSTCA. Each inset in the lower right shows the plate viewed from a different angle.

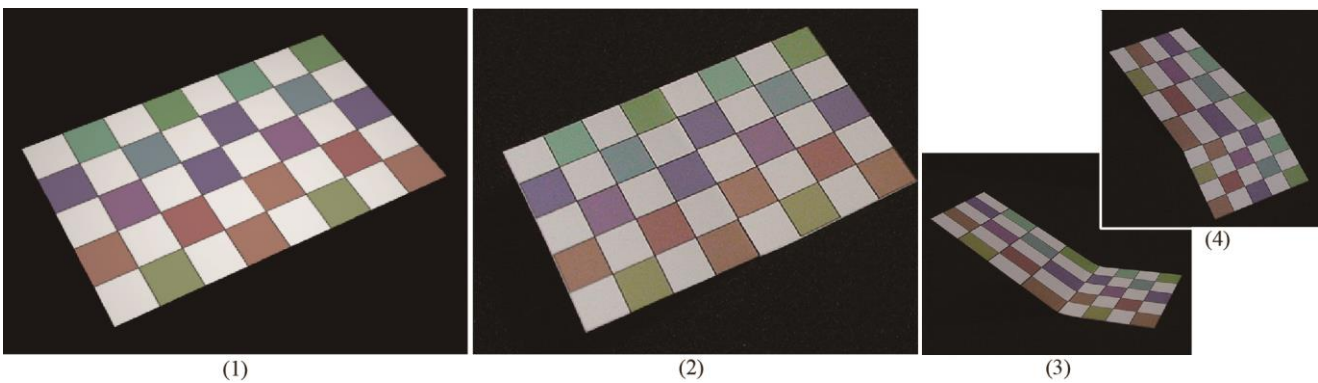


Figure 12: Each plate is texture-mapped under a surface light source. A comparison among the following: (1) apparent surface by CG, (2) actually photographed the mimetic surface after applying MSTCA, (3) and (4) the actually photographed same surface in (2) from different angles.

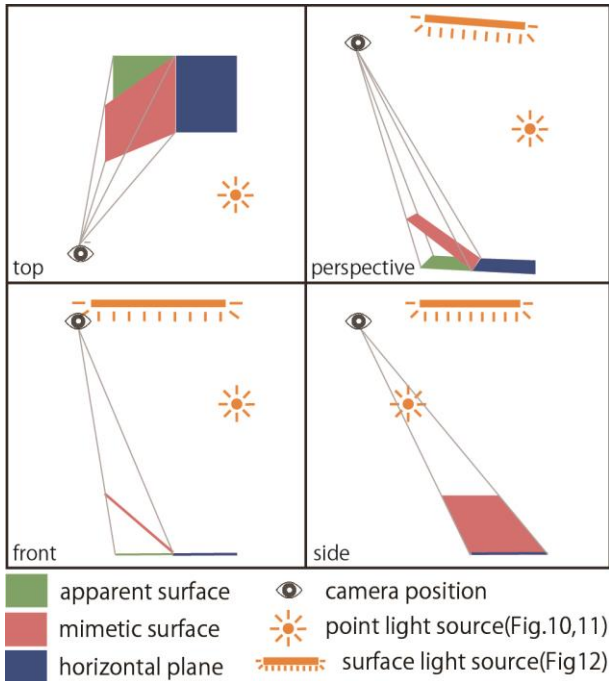


Figure13: Positional relationship is shown by top, front, side and perspective views of Figures 10-12.

3.3 Application Examples

In Figure 10, a point light source is used and each inset at the lower right shows the plate viewed from a different angle. Each plate in 10(1) and (2) is monochromatic blue. The plate in 10(1) is the apparent surface, which is a full horizontal plane. The left halves of the bent plates in 10(2) and (3) are slopes. In 10(2), the plate exhibits a fold line in the middle and it does not appear to be a flat, monochromatic blue plate. In 10(3), the left half of the bent plate is the mimetic surface after applying MSTCA and it is indistinguishable from the apparent surface in 10(1).

In Figure 11(1)–(3), each plate has been texture-mapped under a point light source and it represents the same shapes shown in Figure 10(1)–(3). The plate in Figure 11(2) was obtained using standard texture mapping and it gives an odd impression. The plate in 11(3) was obtained by applying MSTCA and it appears to be natural, and indistinguishable from that in 11(1).

Figure 12 shows the plate after texture-mapping under a surface light source and it has the same shape as that in Figure 11 (2). 12(1) is the CG image and 12(2)–(4) are actual photographic images. The plate in 12(2) is the output from a single-color 3D printer. The textures were adjusted by MSTCA, printed using a 2D printer, and then pasted in precise locations on the 3D printed model. 12(3) and (4) show actual photographs of the plate in 12(2) from different angles. The actual photograph in 12(2) is considerably similar to the CG image in 12(1). This indicates that MSTCA is effective in real space.

The positional relationships among the apparent surface, mimetic surface, camera, and light sources in Figures 10–12 are shown from the top, front, side, and perspective views in Figure

13.

4 Application in Creating Illusion

4.1 Impossible Figure

The MSCTA method is applied to the impossible figure in Figure 3 and the results are shown in Figure 14. The shading and texture mapping are natural. The method is available for various impossible figures.

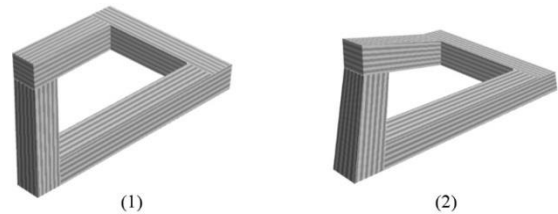


Figure14: The MSCTA method is applied to the impossible figure in Figure 4: (1) from the specified viewpoint, (2) from a different angle.

4.2 Physical Model for Impossible Motion

The following physical 3D model is the output from a single-color 3D printer or constructed of corrugated paper and polystyrene boards. The textures, whose color and shape have been adjusted by MSCTA method, are printed by a 2D printer and then pasted onto precise locations on the model.

4.2.1 Model A

Figure 15(1) shows an actual photograph of impossible Model A. When you focus attention on the slope and stairs, the height of the passageway on the right side differs from that on the left side as shown in 15 (2). However, when focusing on the passageway itself, you can actually see it is on a plane at the same height as shown in 15 (3).

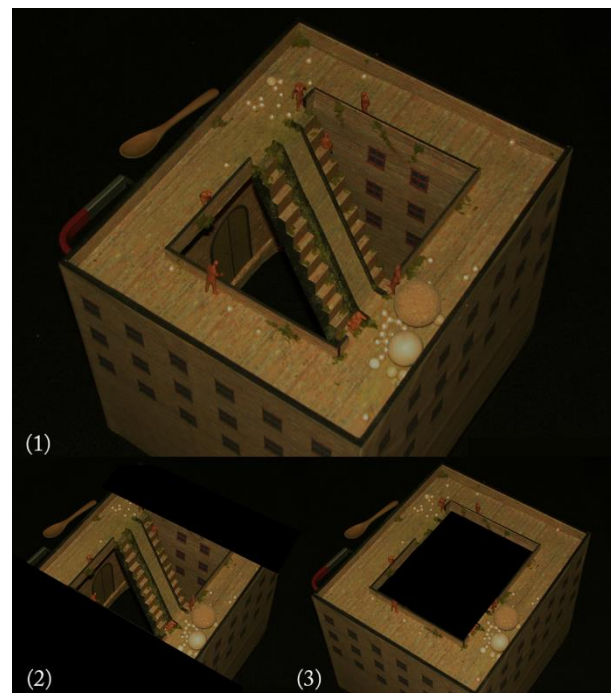


Figure 15: Model A: (1) overall image, (2) focusing on the slope and stairs, (3) focusing on the passageway.

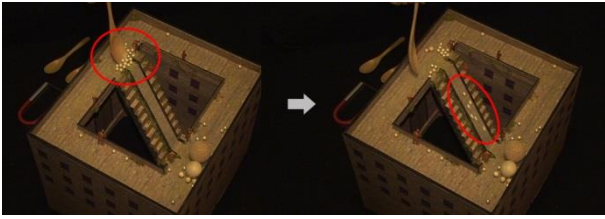


Figure 16: Physical balls which placed on top of the slope roll down due to gravity.

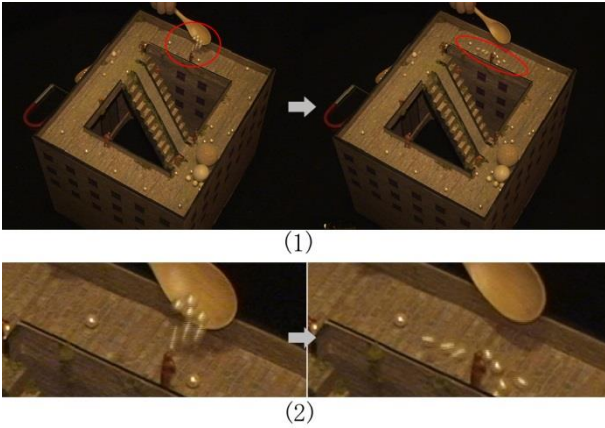


Figure 17: After balls dropped on the passageway, they almost immediately come to a stop: (1) overall images, (2) close-ups of (1).

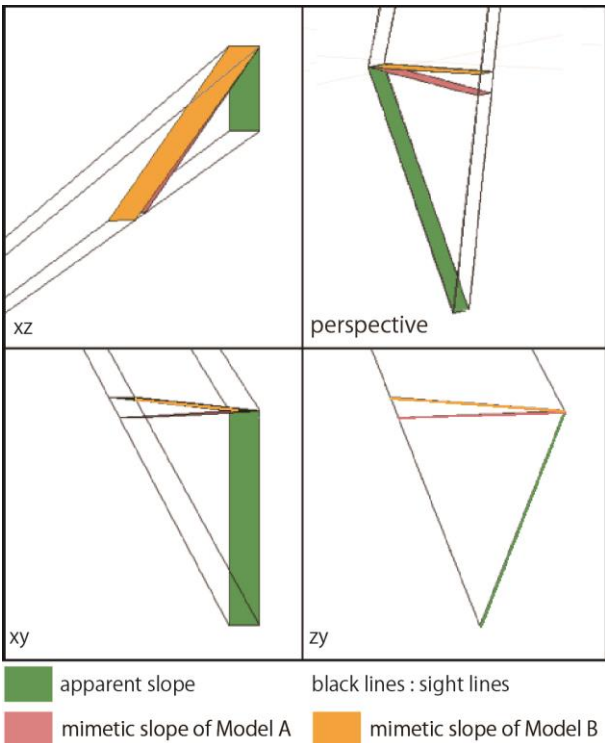


Figure 18: Positional relationship of apparent slope and each mimetic slope of Model A and B

On the physical model, some real balls which placed on top of the slope roll down due to gravity in Figure 16. When some balls are dropped on the passageway, they almost immediately come to a stop in Figure 17. In other words, physical balls on the slope roll down spontaneously, but they on the passageway remain stationary unless acted on by an external force. Thus, not only the appearance of the model but also the movement of the balls is self-inconsistent in height. Its structure is very similar to the one in Figure 13. The part where the passageway is connected to the slope appears to be a horizontal surface, but it is actually a little tilted surface. The slope that looks steep in the middle is actually a gentle slope. Positional relationship of apparent slope and mimetic slope is shown in figure 18. A green polygon is an apparent slope which is steep, a pink polygon is a mimetic slope which is gentle. The overall structure of Model A viewed from two different camera positions is shown in Figure 19. Figure 20 shows a comparison between before and after applying MSTCA at the part where the passageway is connected to the slope on the left side.

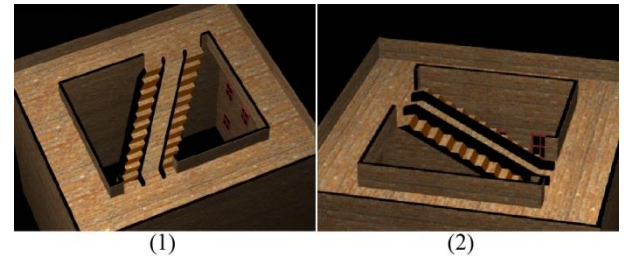


Figure 19: Model A by CG which is viewed from two different camera positions.

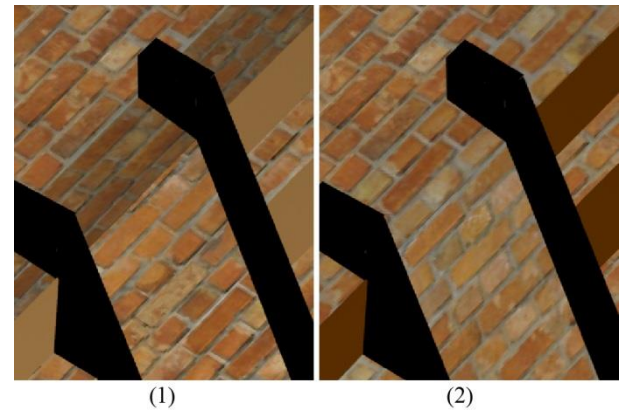


Figure 20: Close-up the part where the passageway is connected to the slope on the left side: (1) before applying MSTCA, (2) after applying MSTCA.

4.2.2 Model B

Figure 21(1) shows Model B appears similar to Model A, but the direction of gravity is reversed along the slope. There is a small square hole in the upper part of the slope. When small balls are moved onto the slope, they roll up the slope by themselves and fall to the bottom through the hole as shown in 21(2). From the direction in which the balls fall, the direction of the gravity becomes clear. When big balls finish going up the handrails of the slope, they arrive at the other side of the passageway as shown in 21(3). The slope that looks appears to

be ascending is descending, as indicated by the orange polygon in Figure 18. The height difference of the slope is less than the height of the handrails. So, big balls can reach the other side of the passageway. Figure 22 shows close-up the slope which is viewed from the side. The hole is lower than the passageway, and the handrails are still higher than the passageway on the left side.

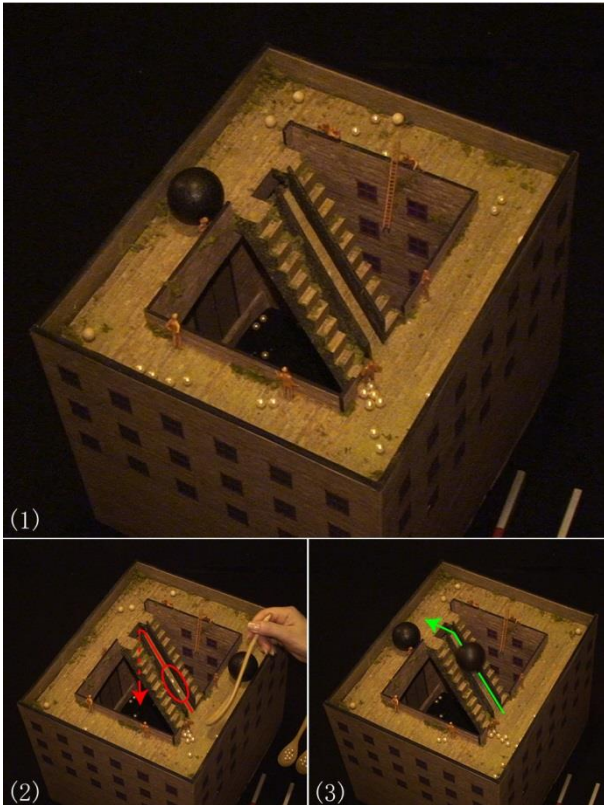


Figure 21: Model B: (1) overall image, (2) red line indicates the trajectory of the small balls, (3) green line indicates the trajectory of the big balls.



Figure 22: The slope of Model B by CG which is viewed from the side.

4.2.3 Model C

In this model, the balls appear to move straight up under the force of gravity as shown in Figure 23. The upper passageway appears to be located straight above the lower passageway. The balls move straight up among the pillars that connect the upper and lower passageways, as if in defiance of gravity. The real figure is tilted sideways and the 'upper' passageway is positioned slightly below the 'lower' passageway. To prevent the balls from spilling out of the tilted model, the side rails of the passageways are deformed to retain the balls, as shown in Figure 24.

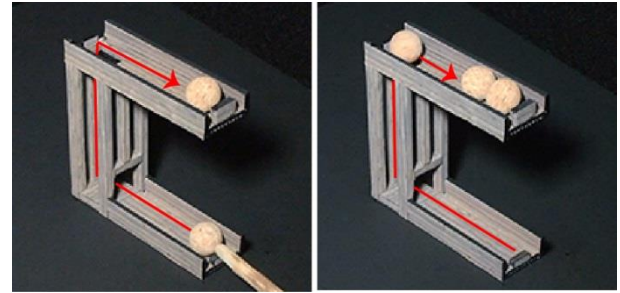


Figure23: Model C: each red line indicates the trajectory of the balls.



Figure24: Side view of Model C.

5 Conclusion

Producing an impossible 3D model that corresponds to a 2D drawing can provide observers with a highly attractive and intriguing experience. In addition, impossible motion is interesting because it occurs in a physical 3D space. To the best of our knowledge, our study provides the first description of textured 3D physical impossible objects based on a consideration of physical light sources. The models obtained using the MSCTA method facilitate more natural expression for impossible objects and the structures have more degrees of freedom when generating impossible motions. At present, 2D printed textures are pasted onto 3D printed models, which have limitations because it is not possible to apply these textures to complex shapes, including curved surfaces. This may be eliminated by the widespread use of full color 3D printers. Thus, we aim to create more rich and expressive artworks by developing this method further.

References

- [1]Seckel A., Masters of Deception, Sterling Publishing Co.,Inc, 2004.
- [2]Penrose L. S, Penrose R., Impossible objects a special type of visual illusion, *British Journal of Psychology* Vol.49 pp.31-33, 1958.
- [3]ERNST, B. Magic Mirror of M.C.Escher, Taschen, 1978.
- [4]Gregory, R. L., The Intelligent Eye, Weidenfeld and Nicolson, 1971.
- [5]Robinson, J. O, The Psychology of Visual Illusion, Hutchinson, 1972.
- [6]Gillam B., Even a possible figure can look impossible, *Perception*, vol.8 pp.229-232 1979.

- [7]Young A W., Deregowski J B., Learning to see impossible, *Perception*, vol.10, pp.91-105 1981.
- [8] Huffman D. A., Impossible objects as nonsense sentences. *Machine Intelligence*, vol.6, pp. 295-323, 1971.
- [9] Clowes M. B. On seeing things. *Artificial Intelligence*, vol. 2, pp.79-116, 1971.
- [10]Cowan T. M., The theory of braids and the analysis of impossible figures, *Journal of Mathematical Psychology*, vol. 11, pp.190-212, 1974.
- [11]Cowan T.M., Organizing the properties of impossible figures, *Perception*, vol. 6 pp.41-56 1977.
- [12]Cowan T.M., Pringle R., An investigation of the cues responsible for figure impossibility, *Journal of Experimental Psychology*, Human Perception and Performance, vol.4 pp.112-120 1978.
- [13]Draper S.W., The Penrose Triangle and a Family of Related Figures, *Perception* vol.7 pp.283-296, 1978.
- [14]Sugihara K., Machine Interpretation of Line Drawings, MIT Press, Cambridge, 1986
- [15]Sugihara, K. Three-dimensional realization of anomalous pictures-an application of picture interpretation theory to toy design, *Pattern Recognition*, vol.30,7, pp.1061-1067, 1997.
- [16]Sugihara K., A Characterization of a Class of Anomalous Solids, *Interdisciplinary Information Sciences*, Vol. 11, No. 2, pp. 149-156, 2005.
- [17]Sugihara K., Computer-aided creation of impossible objects and impossible motions, *Computational geometry and graphtheory : international conference KyotoCGGT*, vol.11, Springer, pp.201-212, 2007.
- [18] Terouanne E., On a class of 'impossible' figures: a new language for a new analysis, *Journal of Mathematical Psychology* vol.22 pp.24-46, 1980.
- [19]Terouanne E., 'Impossible' figures and interpretations of polyhedral figures, *Journal of Mathematical Psychology* vol.24 pp. 370-405, 1980.
- [20]Kulpa Z., Are impossible figures possible, *Signal Processing*, vol.5 pp.201-220, 1983.
- [21]Kupla Z., Putting order in the impossible, *Perception* vol.16 201-214, 1987.
- [22]Uribe D., A set of impossible tiles, *The third international conference Mathematics and Design*, Available at <http://impossible.info/english/articles/tiles/tiles.html>, 2001.
- [23]Simanek. <http://www.lhup.edu/~dsimanek/3d/illus1.htm> 1996.
- [24]Tsuruno S., The animation of M.C. Escher's 'Belvedere', *ACM SIGGRAPH 97 Visual Proceeding*, p237. Presented at Siggraph Electronic Theater, 1997.
- [25]Khoh, C. W., Kovesi P., Animating impossible objects, <http://www.peterkovesi.com/projects/impossible/impossible.htm>, 1999.
- [26]Savransky G., Dimermanz D., Gotsman C., Modeling and Rendering Escher-Like Impossible Scenes, *Computer Graphics forum*, Vol.18, no.2, pp.173-179, 1999.
- [27]Owada S., Fujiki J., Dynafusion: A modeling system for interactive impossible objects, *In Proc. of Non-Photorealistic Animation and Rendering (NPAR)*, pp. 65-68, 2008.
- [28]Orbons E.M.,Ruttkey Zs., Interactive 3D Simulation of Escher-like Impossible Worlds, *Journal of Vacuum Science and Technology*, B - J VAC SCI TECHNOL, B , pp201-208, 2008.
- [29]Wu T.-P., Fu C.-W., Yeung S.-K., Jia J., Tang C.-K., Modeling and rendering of impossible figures, *ACM Transactions on Graphics*, vol. 29, No. 4, article 106, 2010.
- [30]Elber, G. Modeling (seemingly) impossible models , *Computers and Graphics* vol.35, pp.632-638, 2011.
- [31] Lipson A., Andrew Lipson's LEGO, <http://www.andrewlipson.com/lego.htm>, 2002.
- [32]Elber G., Escher for real, <http://www.cs.technion.ac.il/~gershon/EscherForReal> 2002.
- [33]Tabary F., impossible sculptures, http://www.francistabary.fr/index.php?menu=sculptures_impossibles.
- [34]Sugihara, K., Impossible motion: magnet-like slopes, First Prize, Best Illusion Contest of the Year, 2010.
- [35]Tsuruno S., Illusion of Height Contradiction , Top 10 finalists in the 2012 Best Illusion Contest of the Year, 2012.